Journal of Medical Robotics Research, Vol. 0, No. 0 (2013) 1–19


# Cognitive AutonomouS CAtheters operating in Dynamic Environments

E. Vander Poorten[a], P. Tran[a], A. Devreker[a], B. Rosa[a], C. Gruijthuijsen[a], S. Portoles-Diez[a], G. Smoljkic[a], V. Strbac[a], N. Famaey[a], D. Reynaerts[a], J. Vander Sloten[a], A. Tibebu[b], B. Yu[b], C. Rauch[b], F. Bernard[b], J. H. Metzen[b], S. Giannarou[c], L. Zhao[c], S-L. Lee[c], D. Stoyanov[d], E. Mazomenos[d], P. Chang[d], M. Kvasnytsia[e], J. Van Deun[e], E. Verhoelst[e], M. Sette[f], A. Di Iasio[f], G. Leo[g], F. Hertner[h], D. Scherly[h], L. Chelini[h], N. Häni, D. Seatovic[h], H. De Praetere[i], P. Herijgers[i]

[a] *Dept. of Mechanical Engineering, KU Leuven, Celestijnenlaan 300B, 3001 Heverlee, Belgium*
*E-mail: firstâuthor@kuleuven.be*

[b] *Faculty Mathematics and Computer Science, Univ. Bremen, Robert-Hooke-Str.5, D-28359 Bremen, Germany*

[c] *Hamlyn Centre for Robotic Surgery, Imperial College London, Exhibition Road, London, SW7 2AZ, UK*

[d] *CMIC, University College London, Hampstead Road, London, NW1 3EE, UK*

[e] *Materialise NV, Technologielaan 15, 3001 Leuven, Belgium*

[f] *Medyria AG, Technoparkstrasse 2, 8406 Winterthur, Switzerland*

[g] *St.Jude Medical Geneva, Chemin du Grand-Puits 42, 1217 Meyrin, Geneva, Switzerland*

[h] *Zürcher Hochschule für Angewandte Wissenschaften, Technikumstrasse 5, CH-8401 Winterthur, Switzerland*

[i] *Department of Experimental Cardiac Surgery, University Hospital Leuven, 3000 Leuven, Belgium*

Advances in miniaturized surgical instrumentation are key to less demanding and safer medical interventions. In cardiovascular procedures interventionalists turn towards catheter-based interventions, treating patients considered unfit for more invasive approaches. A positive outcome is not guaranteed. The risk for calcium dislodgement, tissue damage or even vessel rupture cannot be eliminated when instruments are maneuvered through fragile and diseased vessels. This paper reports on the progress made in terms of catheter design, vessel reconstruction, catheter shape modeling, surgical skill analysis, decision-making and control. These efforts are geared towards the development of the necessary technology to *autonomously* steer catheters through the vasculature, a target of the EU-funded project CASCADE (Cognitive AutonomouS CAtheters operating in Dynamic Environments). Whereas autonomous placement of an aortic valve implant forms the ultimate and concrete goal, the technology of the individual building blocks that are identified to reach this ambitious goal are expected to be much sooner impacting and assisting interventionalists in their daily clinical practice.

*Keywords*: Robotic catheters; cognitive surgical robotics; fluidic actuation, automatic registration, 3D reconstruction, SCEM, real-time FEM, continuum robot control, teleoperation, haptic guidance, machine learning, autonomous catheter control

## 1. Introduction

Cardiovascular diseases (CVD) form the single most common cause of death in the EU. Catheter procedures are among the most common surgical interventions used to treat CVD. Due to their minimal access trauma, these procedures extend the range of patients able to receive interventional CVD treatment to age groups dominated by comorbidity and unacceptable risks for open surgery.[1–4] The downside associated with minimising access incisions lies at the increased complexity and difficult manipulation of the instruments and anatomical targets. These aspects can be attributed to the loss of direct access to the anatomy and poor visualisation of the surgical site. Steering compliant catheters through a fragile cardiovascular system, under the presence of slack and friction and under disturbances induced by physiological motion is a complex and demanding task. The physical and mental load associated with these procedures could lead to human errors[5] and suboptimal outcome.[6–8] Robotic system developers such as Hansen®

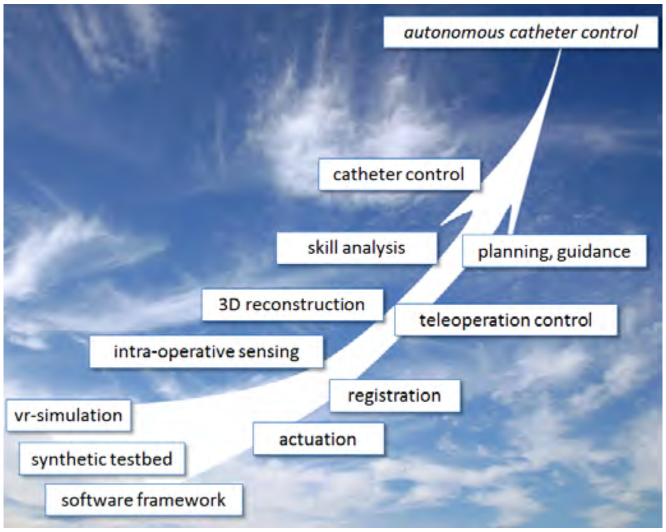


Fig. 1. Building blocks on the way towards cognitive autonomous catheter navigation.

Medical, Stereotaxis® or Corindus responded by offering the clinicians ergonomic workstations from where robotic catheters are steered via teleoperation. While these systems reduce the physical load, improvements are still possible to reduce the mental load of the surgeon, the surgical outcome and the overall level of invasiveness of the procedure.

The CASCADE project is set to develop technology to control catheters in a fully autonomous manner throughout the vessel system. A great number of aspects need to be mastered to this end. Fig. 1 indicates the different elements that have been identified and are elaborated upon in the project. While every element can be seen to contribute to the higher goal, it is believed that progress on individual building blocks could create independent value on a shorter term and improve the quality of robot-assisted, but also manually-executed, interventions. Similarly, although CASCADE focuses on TransAortic Valve Implantation (TAVI), the followed approach and key technology could transfer to other interventions as well.

The paper is structured as follows. After further explaining the clinical application and the case for robot-assisted treatment (Sec.2) an overview of the progress per building block is offered in Sec.3-7. Finally, conclusions and directions for further work are sketched in Sec.8.

## 2. Case for Robot-Assisted TAVI

### 2.1. *Clinical aspects of TAVI*

Aortic stenosis is the most common condition requiring valve surgery in the developed world. The incidence of aortic stenosis is increasing due to an aging population. Only in the US, about 85000 aortic valve replacements are performed annually.[9] When the aortic valve is partially stenosed the strain on the heart muscle increases and the heart function eventually decompensates. Survival rates after the onset of symptoms in severe aortic stenosis are dismal, as low as 50% at 2 years and 20% at 5 years.[10] Surgical aortic valve replacement (AVR) is the current standard of care, but it has been estimated that between 30% and 60% of patients do not undergo AVR, owing to advanced age, left ventricular dysfunction, or the presence of multiple coexisting conditions.[11,12] However, with surgical treatment, the prognosis is excellent if the patient is otherwise in relatively good condition.

Patients with high peri-operative risks that were previously classified as inoperable, can now be operated with Transcatheter Aortic Valve Implantation (TAVI).[1–4] When the transfemoral approach is followed, as depicted in Fig.2, a guidewire, sheaths and catheters are introduced into the femoral artery and navigated through the vessel system. The main function of the guidewire is to find and establish a passage through the remaining opening of the native calcified valve. Typically a certain number of attempts are made to cross the opening. The interventionalist will try to limit the interaction force during these attempts so as to minimize the risk for calcium dislodgement. After the guidewire is put into place a catheter with embedded balloon is advanced by sliding it over the guidewire. When centered at the level of the native valve, the balloon is dilated to create space. A delivery catheter with valve implant is advanced next. The interventionalist will manipulate this catheter so that the implant is aligned perpendicular to and

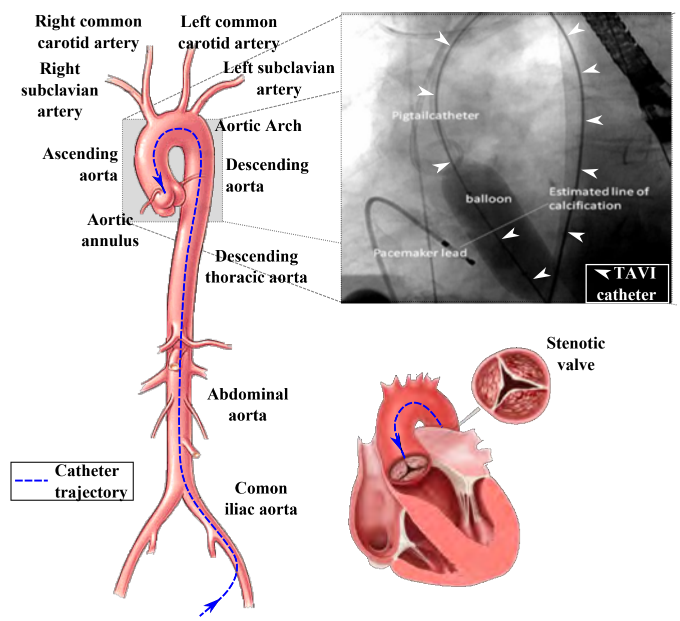


Fig. 2. Transcatheter Aortic Valve Implantation; [left] aortic anatomy, trajectory followed by valve placement catheter; [right-up] fluoroscopic image of aortic annulus, balloon dilation to make place for valve implant; [bottom-right] view upon stenotic aortic valve.

centered with a plane through the aortic annulus. During valve delivery, valve positioning is based on fluoroscopy. Direct visualisation of the native valve itself is here difficult, but due to the nature of the disease, most stenotic valves are calcified. As calcium is visible, the interventionalist may infer the position of the valve and the annulus from observing the calcium. Additionally, angiography dye may be injected to clarify the valve position. Depending on the manufacturer of the valve implant the valve is self- or balloon-expanded. Care is taken to keep the implant well-aligned during this expansion. During the implantation the heart is typically arrested for this purpose.

Transfemoral TAVI is less invasive for the patient than an open procedure or a transapical approach, but presents considerable challenges and risks for surgeon and patient:

- operation under low-quality two-dimensional view with limited soft-tissue discrimination;
- patient and surgeon are exposed to ionizing radiation from imaging;[13] the contrast agent that is used to improve visualisation is demanding for kidneys and could cause allergic reactions;[13]
- bad controllability of catheter; limited bandwidth due to slack, friction, and catheter compliance;
- little control over interaction forces, possibly causing dislodgement of plaque or calcium, tissue damage or rupture;[14,15]
- lengthy procedure involving many preparatory steps including the introduction of a guidewire, of a catheter to dilate the native valve, of a stabilizing sheet and so on;
- safety issues arise as the surgeon is working in a non-ergonomic manner under high mental and physical load.

Interventionalists especially experience problems in finding and crossing the opening into the native calcified valve.

- While attempting to cross the native valve undesirable and intense contacts could arise, resulting in dislodgement of plaque or calcium that, taken up in the blood circulation, could end up in the brain and result in stroke;[8]
- to simplify crossing of the valve rapid pacing is applied to arrest the heart temporarily, which should be cautiously used and kept short ($\leq 15s$ according to Webb *et al.*[16]);
- care must be taken that during the placement the implant is well aligned and does not migrate inside the heart or towards the coronaries. When inadequately positioned the risk for damaging the heart muscle or blocking the coronaries grows. Morena *et al.* reported an overall mortality during the procedure of 2.3%;[6]
- if the cathether and associated valve is badly oriented this may lead to paravalvular leakage.[7]

### 2.2. *Objectives for robot-assisted TAVI*

While some of abovementioned issues are addressed by state-of-the-art robotic technology;[17,18] existing commercial solutions such as those provided by Hansen® Medical, Corindus or Stereotaxis® are neither intended for TAVI nor fit for such dynamic and precise control.[17] From discussions with clinicians the following needs were established. A solution is needed (a) dedicated to TAVI, preferably offering broader use in other catheter procedures; (b) that is less dependent on damaging imaging techniques such as those relying on x-ray or contrast agent; (c) offers improved awareness of and control over the interaction between catheter and vasculature; (d) allows more detailed control of the catheter tip, leading to an improved valve positioning and alignment quality. (e) cuts down in execution time, e.g. by omitting the use of a guidewire; (f) releaves the need for rapid-pacing to arrest the heart and that (g) offers more ergonomic operation, reducing both physical and mental workload. To address these clinical needs, in accordance with the basic vision expressed in Fig.1, CASCADE works to progress the following key technologies:

- catheter actuation (SubSec.4.1);
- intra-operative sensing (SubSec.4.2);
- intra-operative modeling (Sec.5);
- skill analysis and planning (Sec.6);
- advanced robotic control (Sec.7),

towards a new type of *cognitive* catheter that is able to *autonomously* navigate through the vessels and, in the envisioned use case, is capable to adequately position and align valve implants. A dedicated software framework and carefully engineered virtual and synthetic test-beds, discussed in Sec.3, form key enablers to support and speed up the development in this highly interconnected task.

## 3. CASCADE software framework, virtual and synthetic test-beds for prototyping catheter-based interventions

This section briefly describes the CASCADE software framework (SubSec.3.1), the virtual reality (SubSec.3.2) and synthetic test-beds (SubSec.3.3) that have been developed to facilitate deployment and prototyping of the different hardware and algorithms. These building blocks are key for structured and efficient development and validation.

### 3.1. *CASCADE software framework*

Fig.3 introduces the software framework that has been built by the system integrators.[19] The framework was designed addressing two major types of users. At one side it provides the environment and tools to support efficient software development and prototyping; at the other side it serves as the main interface to interventionalists who now receive access to a vast amount of data including clinical data, sensory, possible steering actions, guidance keys that must be handled with. In close collaboration with the clinicians and the developers the specifications for the different visualisers and interfaces have been defined, evaluated and refined.

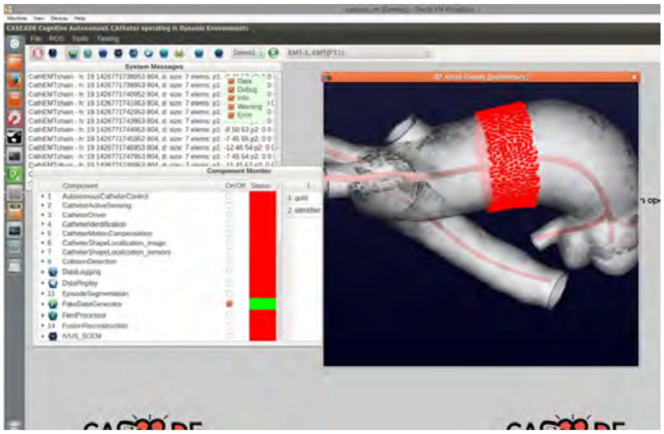

Fig. 3. View upon CASCADE development environment: [left] software components and functionality can be switched online. Developers have access to raw data and communication signals. [right] user interface, different visualisers can be selected to assist in catheter steering or planning. The Aorta3DViewer shown here displays the active 3D mesh, the aorta centerline. Parts of the mesh selected for finite element analysis are highlighted.

To ensure reliable control and timely operation of components and catheters the framework is designed following a component-based philosophy. All functionality is encapsulated in loosely coupled components. The ROS messaging system is used to communicate between components. Components that require hard real-time operation rely on OROCOS for correct and timely functioning.

The system design follows a three-tier architecture, whereby components are allocated to one particular tier. This enables a clear and logic separation of system parts. The interface, depicted in Fig.3, supports efficient software development and debugging. Components can be switched on and off on the fly allowing quick configuration of the system for any particular test.

An abstraction layer is installed making abstraction of the actual hardware components that are being used. In fact, software components are ignorant as to whether they are communicating with a real catheter and testbed or with a *virtual* one described in next SubSec.3.2. It is good practice to consistently validate algorithms in the virtual reality system before directing the communication to the hardware to conduct real-world experiments.

### 3.2. *Virtual Reality Environment*

While the catheter is inserted into the vasculature, it flexes, bends and adapts its shape to the surrounding vessel. The overall interaction with the vessel is highly complex and cannot be captured by a simple set of analytical formulas. A virtual reality environment has been built to simulate this behaviour and speed up development and testing. Compared to real-world experiments, simulations in a virtual environment are more practical as they hardly require setup time. Data can be logged, replayed and analysed. Experiments can be repeated as much as needed, exotic scenarios can be simulated easily. Of strategic importance is the availability of ground-truth information which allows unambiguous verification of performance of algorithms. The realism of the simulation environment is of course crucial as it determines the confidence one can attach to analyses that have been conducted.

Different algorithms have been proposed in the literature to simulate guidewire or catheter behaviour. Methods have been proposed based on mass-spring models,[20,21] the Finite Element Method[22] or discrete versions of the Elastic Kirchhoff Rod theory.[23,24] CASCADE progresses the work by Konings *et al.* who predict the behaviour of a guidewire by minimizing the joint energy of guidewire and surrounding vessel.[25–29] The underlying idea is that since the overall motions are relatively slow, a quasi-static approximation of the catheter/vessel complex is justifiable. Under this assumption the catheter comes at rest in an equilibrium state after each simulation step. The shape it will take on is one where the aggregated energy (of catheter and vessel) is minimal. The algorithm of Konings *et al.* was expanded towards catheters featuring multiple active DoFs. It was used amongst others for prototyping novel catheters, generating data-sets for machine-learning, but also for user tests and catheter control experiments.[30–32] Figure 4 gives a view upon the virtual reality simulation environment that was developed featuring apart from a 3D-viewer a.o. a fluoroscopy viewer providing familiar images to the clinicians.

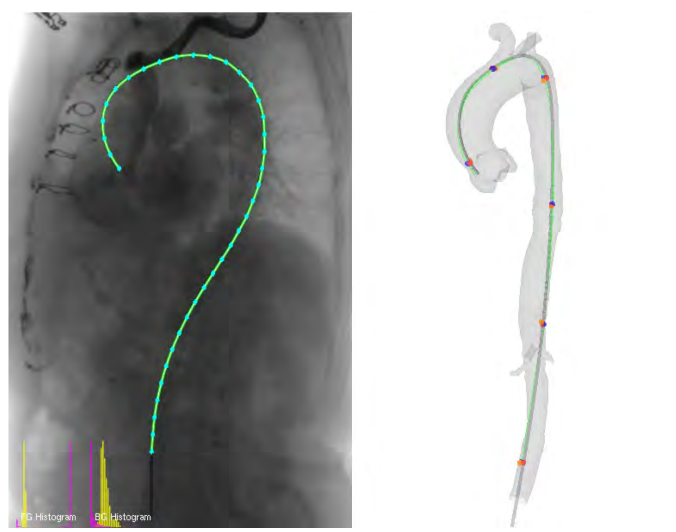


Fig. 4. Virtual reality simulation environment developed within CASCADE, used for rapid prototyping of novel catheters and algorithms. In the present view, sensor-based reconstruction of the catheter shape (green line) is evaluated by comparison with the simulated ground-truth (black/grey line). [left] fluoroscopy viewer - [right] 3D viewer of catheter in aorta.

### 3.3. *Development of synthetic perfused test-bed*

A higher level of evidence or confidence is associated with real-world experiments. Both from an ethical viewpoint as for practical reasons it is opportune to invest in the development of dedicated synthetic testbeds to validate algorithms and hardware. Requirements for such testbeds are:

- accurate vessel geometry - containing ascending aorta with left and right coronary artery bifurcation, aortic arch with brachiocephalic, left common carotid and left subclavian artery, abdominal aorta with mesenteric, left and right renal and common iliac artery;
- realistic mechanical properties, resulting in typical natural catheter behaviour and vessel deformation under physiological phenomena and catheter interaction;
- possibility to simulate risk prone areas such as aneurysms or calcification;
- compatibility with novel catheters and sensors; a.o. with MR, CT, electromagnetic tracking and ultrasound;
- good transparency, allowing visual confirmation of the catheter and the use of cameras to simulate fluoroscopy.

To meet the requirements several testbeds were engineered as summarized in Table 1. All testbeds were built from real patient data. CT data was segmented using the Mimics Innovation Suite® (Materialise NV). This data was also used in the VR environment (SubSec.3.2) allowing comparison and transfer of learned knowledge.

Rigid 3D models were made from stereolithography (SLA, wall thickness 2 mm, surface smoothing and cosmetic finishing step, Fig.5.a,b). 95% of the surface elements were confirmed to lie within an interval of $[-0.5, 0.5]$ mm from the original model. So the CAD data could be used as a ground truth for the geometry of this model.

Table 1. Summary synthethic test-bed properties prepared in CASCADE, legend: [×] pass; [o] borderline; [ ] not investigated

| | | full aorta | deformable | robust | transparency | US compatible | calcification |
|---|---|---|---|---|---|---|---|
| SLA | Fig.5.a/b | | | × | × | × | |
| HeartPrint™ | Fig.5.c/d/e/f | × | × | o | o | × | × |
| HybridSiliconCast | Fig.5.g | × | × | × | × | × | |

For more advanced experiments deformable models were used. A first set was printed from HeartPrint™Flex (wall thickness 1.5 mm). The mechanical properties approach those of the human vasculature[33] as was verified through uniaxial tensile tests. Utilizing multimaterial inkjet, 3D printing calcifications can be incorporated into this model (Fig.5.e). Additionally, the model showed excellent US compatibility. Fig.5.f shows also the calcification clearly. However, the robustness of this material was restrictive for the purposes of CASCADE, where unlimited passage of catheters is required. Therefore a modular setup was made (Fig.5.c/d) to easily replace damaged parts. In parallel, a novel hybrid silicon casting technique was developed showing superior robustness and excellent transparency (Fig.5.g), good ultrasound compatibility and mechanical properties. Embedding calcifications is less straightforward and was not attempted at this point.

A dedicated perfusion system is built and connected to the synthetic vasculature. Water with added Calcium is used for perfusing, not jeopardizing the visibility and at the same time offering good ultrasound properties and low friction. A support was designed to provide anatomically correct positioning of the testbeds, yet allowing realistic deformation and motion of the testbed upon perfusion, replicating physiological motion from heartbeat and breathing.

## 4. Self-aware dynamic catheters

Excellent dynamic properties are needed in order to precisely align a valve implant while the heart is still beating (SubSec.4.1). Also, good knowledge of the own pose (shape) with respect to the surrounding vasculature helps determining appropriate steering actions. This section describes the progress in catheter development towards catheters that can safely operate in dynamic and deformable environments such as the vasculature. Reducing the dependency on damaging imaging techniques could be done by making the catheter *self-ware* which would imply embarking intra-operative sensors to the catheter (SubSec.4.2).

### 4.1. *Fluidic actuation*

Traditional cable-actuated catheters suffer from friction and non-isotropic behaviour. These effects complicate dynamic coordinated control of the distal degrees of freedom (DoFs) and make it difficult to maneuver the catheter precisely in fragile and dynamic environments such as in the vicinity of the aortic annulus.[34] Several researchers have looked into catheter control in a dynamic context. Kesner *et al.* introduced an approach for mitral valve repair featuring motion-compensation to account for heart beat.[35,36] The said system is appealing, yet only deals with a single DoF, thus not allowing adjustment of the orientation. Vrooijink *et. al.* proposed a robotic delivery sheath for transapical TAVI.[37] Similar to traditional commercial robotic catheters, its tip is articulated by two pairs of antagonistic tension wires. Friction and backlash within the system limit the dynamic range. This limitation will be even more pronounced when moving towards transfemoral TAVI. Shape Memory Alloy (SMA)-based solutions[38,39] also have limited dynamic response due to the thermo-mechanical phenomena involved. SMA actuation compares

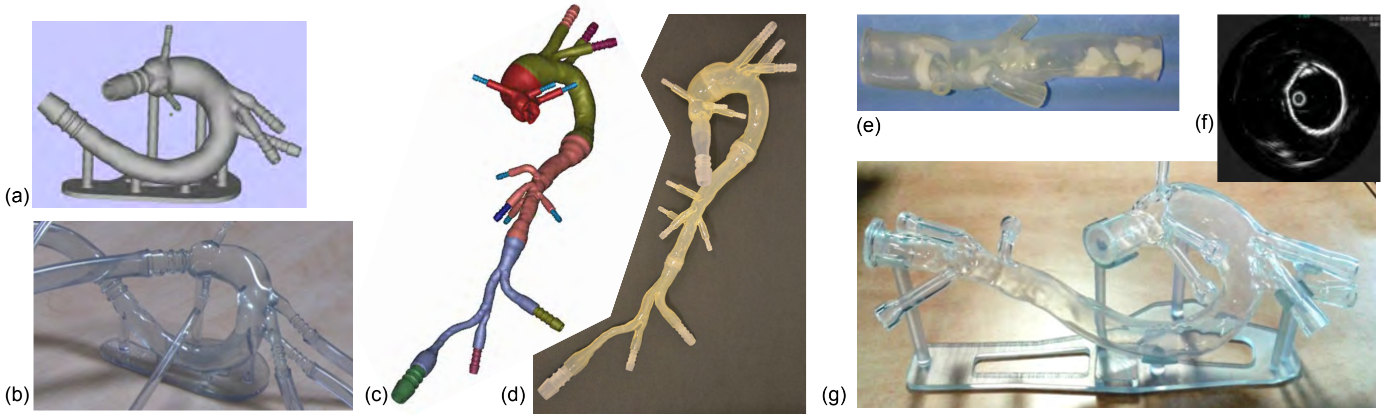


Fig. 5. View upon 3D printed testbeds - (a)/(b) CAD and printed rigid SLA model; (c)/(d) CAD and printed HeartPrint™Flex model; (e)/(f) multimaterial inkjet 3d printing with HeartPrint™and IVUS image. Calcifications visible in (e) appear clear in corresponding IVUS image (f); (g) Aorta model by new hybrid silicon casting technique showing good transparency and flexibility.

favourably to cable-based approaches when many active DoFs are needed. As the number of cables rises latter catheters become increasingly stiff, making it easier to damage surrounding tissue. For a fairly recent survey of robotic catheters please refer to Fu *et al.*[40] Fluidic actuation, as introduced by Ikuta *et al.*, is among the more appealing approaches as the associated compliance offers a certain level of intrinsic safety.[41] At the same time raising the number of DoFs does not necessarily imply that the catheter becomes prohibitively stiff. Keeping the overall dimensions low is a challenge though. Whereas, Ikuta made use of a series of bellows supplied by a single pressure line, the authors have been developing more powerfull fluidic catheters employing McKibben muscles.[42]

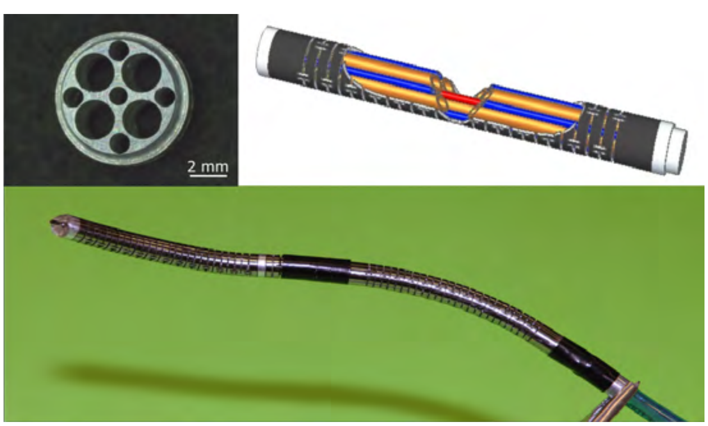


Fig. 6. Picture and CAD design of distal section of fluidic actuated catheter and connector;[42–44] four antagonistic McKibben muscles inside a nitinol structure that acts as return spring.

The Virtual Reality environment has been used to determine appropriate location, length and bending characteristics of the muscles for integration in a catheter for TAVI.[30] The muscles were built in-house and integrated into an outer nitinol backbone structure forming an active bending element. Fig. 6 shows the distal part of a with two 2DoF bending segments. The actuator bandwidth was found to exceed 8Hz.[44] The displayed catheter has 7mm outer diameter whereas 6mm is the indicative diameter provided by the clinicians. Since then,[42,43] new muscles have been designed with similar or better bending properties only requiring 1.2mm diameter. This opens perspectives for further catheter miniaturisation.

## 4.2. *Intra-operative sensing*

As the vasculature is compliant and subjected to deformations from physiological phenomena (heartbeat and breathing), but also undergoes deformation by the insertion of guidewires and catheters, it is dangerous to rely solely on pre-operative data for navigation. In clinical practice interventionalists rely on fluoroscopy and on injection of contrast agent to get a better sight on the anatomy of the vasculature. In order to reduce the dependency on fluoroscopy it is possible to embed relevant sensors directly into the catheter. Based on intra-operative sensing up-to-date models of the catheter and the surrounding vasculature can be built; the topic of section 5. A distinction is made between sensors for proprioception (subsection 4.2.1) and those for exteroception (subsection 4.2.2).

### 4.2.1. *Sensors for catheter proprioception*

A good understanding of the entire 3-dimensional catheter shape is essential for taking sensible navigation decisions and e.g. avoid risk-prone areas. A convenient way to achieve such proprioception or *shape sensing* would be by means of a set of electromagnetic tracking sensors (EMT, Aurora, NDI Medical). A number of miniature sensors could be distributed over the catheter length. In CASCADE for example an EMT sensor is integrated at the catheter tip (Aurora Micro 6 DoF, 0.8mm O.D, Fig.7(a)), at convenient distances along the catheter length other sensors (5 Aurora 5 DoF sensors, 0.5mm O.D) are integrated. The EMT sensors measure their (and thus the catheter's) pose at 40 Hz, with a precision of about 0.9 mm and 1 deg within the field generators's working volume. An adequate distribution of EM sensors was found through simulation in VR. Recent shape sensing technology (Fig.7(e)) based on fiber bragg grating[45] bears great promise,[46] but is still costly.

#### 4.2.2. *Sensors for exteroception*

To observe the vasculature from within the vessel one could make use of IntraVascular UltraSound (IVUS) sensors. For example the Visions PV.035® (Volcano Corp., CA, USA) provides a 30mm radius cross-sectional view at 20Hz update rate of the vessel along a section perpendicular to the probe. Forward Looking IVUS probes (FLIVUS) would be a great use as well, but are still under development[47] and are not yet available commercially. The flow gives additional information about the relative pose w.r.t. the vessel wall. For example flow meaurement could be a contact-less approach to reveal the opening into the calcified valve. Fig.7(d) gives a view on a catheter with flow sensor (TrackCath, Medyria AG) that has been used within CASCADE.

Force sensing could further improve safety and awareness of the environment. Especially at the catheter tip large contact stresses could occur, possible causing tissue damage, vessel rupture or calcium dislodgement. A fiber optic tri-axial force sensor (TactiCath™, SJMG, 3.5mm O.D., 1g resolution, 7(b))) based on the Fabry-Perot principle is a commercially available solution that was used.

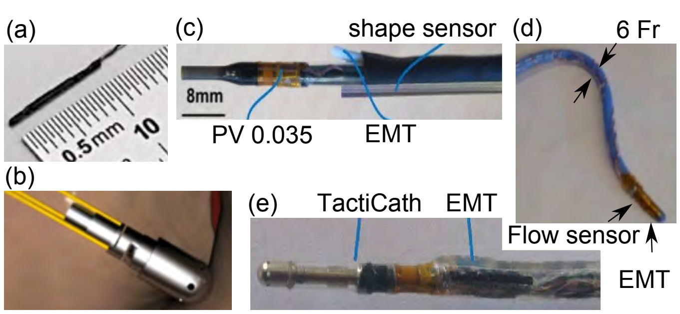


Fig. 7. Selection of sensors/catheters for intra-operative measurement (a) 6DoF EMT sensor (Aurora® NDI); (b) TactiCath™; (c) catheter with IVUS and EM; (d) Flow sensing catheter w. embedded EMT; (b,e) force-sensing catheter w. EM.

## 5. Intra-operative modeling

Self-aware catheters acquire timely, possibly more detailed information about the inside of the vessel. By using this information it becomes possible to provide additional insights and enhance the user or controller's awareness of the catheter/vessel system. This could potentially lead to more appropriate and safer navigation. The different intra-operative modeling techniques described in the following are examples of how the intra-operative (intravascular) sensing could be exploited advantageously.

### 5.1. *Automatic registration of pre-operative data*

A first obvious expansion of current surgical practice would consists in making better use of the pre-operatively acquired MR/CT data to augment the limited two-dimensional images obtained from fluoroscopy. The additional contextual information would help planning future actions. For this to work both datasets need to be aligned or *registered* properly. A review of the basic registration schemes is provided by Sra *et al.*[48] Current registration methods, including those applied on catheter procedures,[49–51] require a significant amount of human interaction. As this is both time-consuming and error-prone these methods are hardly applied in clinical practice. To more readily integrate the registration process into the surgical workflow, it is desirable to have *automatic registration*, where user involvement is limited to supervision.

Through the use of catheters with intra-operative (intravascular) sensing capability becomes possible. For example in earlier work, Zhong *et al.* used IVUS to automatically collect a dense point cloud[52] that is then registered to the pre-operative data using the Iterative Closest Point (ICP) algorithm. While reducing the efforts for registration, user interaction is eliminated with Zhong's appraoch. This is because ICP is sensitive to outliers and requires a suitable initial registration guess to work properly.

Data from the sensors attached to the catheter, as described in 4, are used to facilitate automatic registration of pre-operative MR/CT images. A fast, global registration algorithm is proposed[53] that is entirely automatic and could run continuously in the background spawning updates and improvements at regular intervals. The proposed algorithm is a branch-and-bound stochastic algorithm adapted from Papazov *et al.*[54] The pre-operative MR/CT data is preprocessed and the Euclidean 3D distance transform is computed for the voxelized mesh. The branch-and-bound algorithm is applied next. The sampling method is refined to get a more uniform sampling of the transformation space. Also the cost function is adapted. In order to quickly and safely obtain sufficient intra-operative data on the vasculature for performing an accurate registration we propose not only to consider the *surface points*, i.e. the points located on the vessel wall, but also

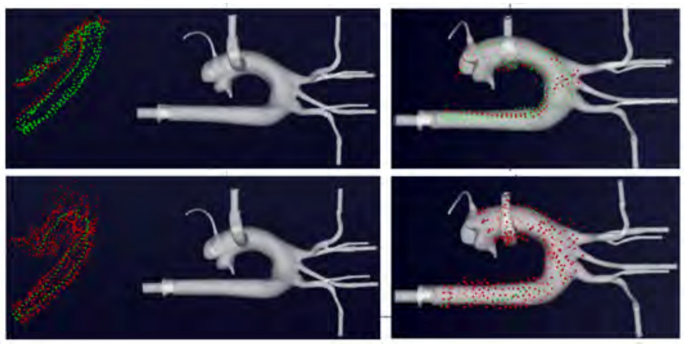

Fig. 8. Data-to-model registration result for (upper row) EMT-force catheter, and (lower row) EMT-IVUS catheter. Surface points are depicted in red and lumen points in green.

to account for *lumen points*. These are measurement points of the catheter itself that do not contact the vessel wall. Under the assumption that the catheter does not depart from the vasculature these points provide information about the location of the vessel lumen.

In the case of a sparse set of surface points, the proposed registration algorithm[53] is able to double the registration accuracy thanks to these lumen points. The algorithm has been validated on the synthetic aorta model described in SubSec.3.3. Fig.8 shows the result of the registration algorithm using EMT sensors (identifying surface points and lumen points) and IVUS and force sensing (identifying only surface points) respectively. The total global registration process achieved an average registration error of 3.9 mm after 4.8 s computation for a catheter equipped with force and EMT sensors, and of 5.1 mm in 7.4 s for a catheter with embedded IVUS and EMT sensors. This is comparable to accuracies needed for clinical application, as reported by Dong *et al.*[50] The computation time is limited to a few seconds, and no time is added due to the registration process itself, since it does not interfere with the clinical workflow.

### 5.2. *Catheter shape reconstruction*

Knowledge of the entire 3-dimensional shape of the catheter could help planning and assessing risks associated with future steering actions. At present interventionalists rely on conventional monoplane fluoroscopy for online estimation of the catheter shape. Apart from the exposure to radiation and dependency on contrast agent, all depth information is eliminated. Thanks to the EMT sensors that are embedded along the catheter length an online 3-dimensional estimate of the catheter shape can be obtained.

A first method makes use of a series of 5-DoF EMT sensors embedded along the catheter length. These sensors provide pose information at discrete locations along the catheter body, which through a nonlinear cubic spline fitting, gives a 3-dimensional estimate of the catheter shape. The objective function used in this fitting tries to minimize the pose error, maintain the known distances between the sensors (assuming incompressibility along axial catheter length) and reduce the overall bending energy of the resulting curve. Figure 9 shows an example of EMT-based shape reconstruction in the VR environment. Note that when inserted deeper into the aorta, the error rises at the proximal part of the catheter, whereas prediction accuracy at the distal part remains of acceptable quality.

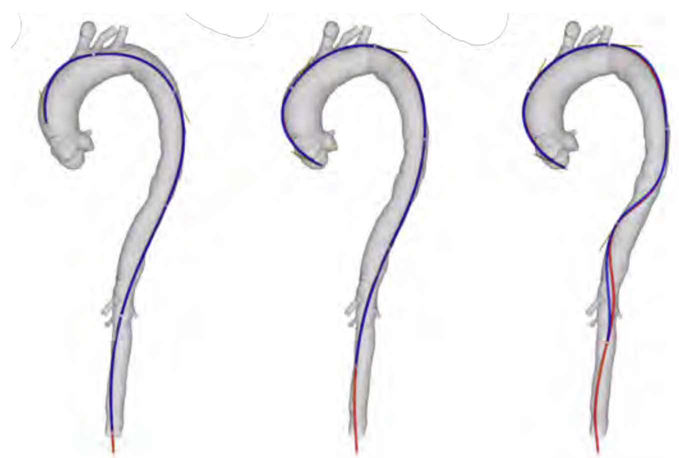

Fig. 9. EMT-based shape reconstruction during virtual catheter insertion; red curve showing ground-truth. The reconstruction RMS errors and Hausdorff errors are respectively [left] $e_{\rm rms}$=0.46mm, $e_{\rm h}$=1.34mm, [center] $e_{\rm rms}$=0.61mm, $e_{\rm h}$=1.41mm, and [right] $e_{\rm rms}$=1.61mm, $e_{\rm h}$=4.39mm.

A second approach fuses EMT data with a catheter tracking algorithm based on fluoroscopy. The main rationale is that if fluoroscopy is present anyway, its use can at least be reduced to anatomical risk-prone areas where a highly accurate and reliable reconstruction of the catheter shape is required. Using a B-spline tube model[55] within a probabilistic framework derived from Bibby *et al.*'s work,[56] the 2D dense information extracted from fluoroscopic images is combined with the 3D discrete pose of the EMT sensors. In constrast to fluoroscopy-based sensing, the fused approach offers a full 3-dimensional catheter shape estimate. On the other hand, compared to pure EMT-based shape sensing, the fused approach is to show greater robustness and accuracy, as the reconstruction algorithm becomes less sensitive to internal and external electromagnetic interferences. It relieves the need of using dedicated shielding or performing tedious calibration procedures that aim to compensate for electromagnetic field distortion errors[57,58] do not integrate well with the current surgical workflow. Promising results for the second approach were obtained from CASCADE's VR simulation environment as shown

Table 2. Evaluation of shape reconstruction errors [mm] using EMT-based and fusion approaches for different catheter insertion lengths $L$ [mm] and number of EMT sensors in VR simulation.

| $L$ | # sensors | $e_{rms,emt}$ | $e_{rms,fus}$ | $e_{h,emt}$ | $e_{h,fus}$ |
|---|---|---|---|---|---|
| 175 | 3 | 1.17 | 0.59 | 1.52 | 0.88 |
| 275 | 4 | 2.06 | 1.68 | 3.96 | 3.40 |
| 385 | 5 | 2.76 | 2.31 | 4.46 | 4.43 |
| 485 | 6 | 1.56 | 0.88 | 3.24 | 1.79 |

in Fig.4. Table 2 summarizes the RMS and Hausdorff distance between the simulated ground-truth and the reconstructed catheter using respectively the first ($e_{rms,emt}$,$e_{h,emt}$) and the second ($e_{rms,fus}$,$e_{h,fus}$) approach. Note that white noise with standard deviation of 1.5mm was added to the virtually generated EMT sensor data in order to simulate electromagnetic disturbances.

### 5.3. *Intra-operative geometric environment modeling*

Whereas the methods from SubSec.5.1 and SubSec.5.2 already reduce the dependency on X-ray fluoroscopy and contrast agent, they do not yet exploit the full potential of intra-operative sensing. Inspired by robotic techniques such as SLAM (Simultaneous Localisation and Mapping) whereby without any prior knowledge a robot moves through its environment and incrementally builds up a 3-dimensional map of its surrounding, CASCADE introduces SCEM: 'Simultaneous Catheter and Environment Mapping'.[46] SCEM is a robust and real-time vessel reconstruction scheme for endovascular navigation based on IVUS and EM tracking. The concept is similar to SLAM, the catheter moves up from the groin, scans the environment - the surrounding vessel - by using IVUS and stitches the obtained 2-dimensional scans to each other to form a 3-dimensional representation of the vessel wall. In principle, a full up-to-date reconstruction of the vessel could be done in such manner completely eliminating the need for fluoroscopy.

A number of processing steps, depicted in Fig.10, are necessary to reliably extract the vessel contour out of the raw IVUS image. Once the contour is obtained, it can be expressed in the absolute coordinate frame of the EM field generator through a simple kinematic transformation (an EMT sensor positioned within the lumen of the IVUS sensors provides the absolute pose of the US probe). Scans can then be stitched to form a closed 3D vessel model.

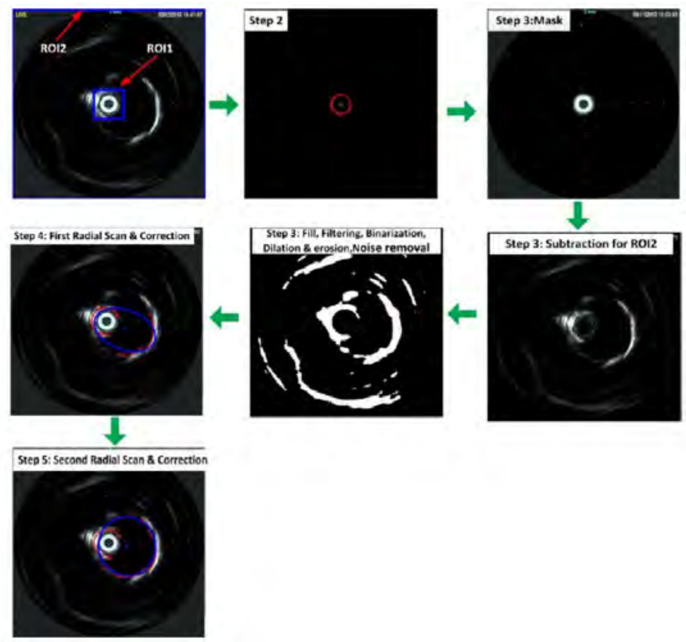


Fig. 10. Different processing steps to extract the geometry of a cross-section of the vessel wall out of an IVUS image. The obtained scan is stiched subsequently to previous scans to obtain an intra-operatively obtained geometric vessel model.

Whereas the earlier methods treated observations from IVUS and EM as exact,[46] the newer methods take uncertainty into account. This allows reduction of the method's vulnerability to errors in the observations and abrupt catheter motion. The latest method first extracts from the IVUS image the contour which represents the inner cross section of the aorta. Then, the vessel reconstruction is formulated as a nonlinear optimisation problem by considering both the IVUS contour and the EM pose as observations, as well as pre-operative vessel morphology. By considering the errors and its corresponding uncertainty of the measurements in the optimisation, the proposed SCEM algorithm is more robust and accurate. Especially in the presence of abrupt catheter motion a significant improvement can be noticed. The experiments on the testbed of which the outcome is depicted in Fig.11 show that the proposed SCEM algorithm results in a much smoother reconstruction.

### 5.4. *Mechanical modeling*

Up-to-date geometric vessel models only capture part of the interaction between the vessel and the catheter as they do not provide a measure of the forces that are exerted. If stresses incurred upon the vasculature are too high this could lead to dangerous situations: tissue damage, vessel rupture, dislodgement of calcium or atherosclerotic plaque.[14,59]

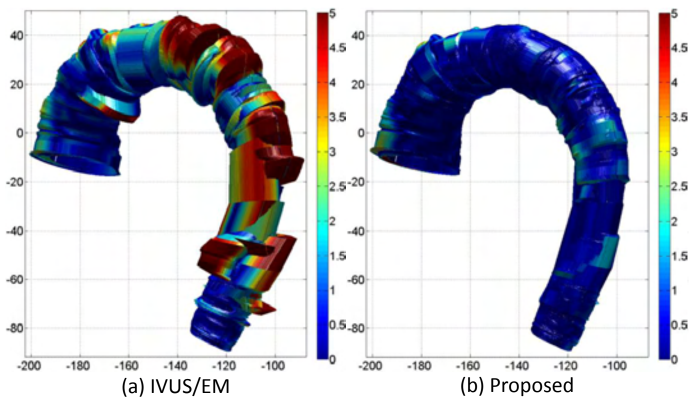


Fig. 11. 3D vessel reconstruction results with abrupt catheter motion (errors in mm); (a) previous implementation[46] - (b) current version considers uncertainty and pre-operative vessel morphology

Through Finite Element Modeling (FEM) of both the vessel and the catheter it would be possible to get an improved understanding of these aspects. Within CASCADE efforts have been paid to allow real-time evaluation of finite element aorta models for intra-operative use. Which such technology interventionalists could re-plan actions and e.g. retract the catheter when observing rising stress levels. Similar, advanced control schemes could automatically limit the interaction forces while steering or following trajectories that give rise to lower stress.

Creating a real-time FEM model of the vasculature is far from trivial. Starting from a general approach by Gregson *et al.*[60] several attempts and modifications were made to generate a high-quality hexahedral mesh of the aorta. While the minimum element quality was improved substantially (scaled Jacobians higher than 0.1), this was found still insufficient for proper use. Further improvements are needed. A general purpose graphics processing unit (GPGPU) implementation of the Total Lagrangian Explicit Dynamic (TLED) algorithm[61] for soft tissue FEM simulation was then made[62] as it possesses good parallellization potential. Fiber reinforced nonlinear constitutive models[63] necessary for simulating aortic tissue were implemented and tested in the TLED. Despite its efficient implementation this FEM analysis is computationally intensive, hence a method was designed to allow fast online selection of a specific region of interest of the aorta. Clearly the area around the catheter tip is of particular interest as large stresses could easily develop between the tip and the vessel. Fig.3 shows the result of a selection around the tip region. In addition, a global deformation algorithm was developed. Based on an updated aorta centerline that could e.g. be obtained as an outcome of the SCEM algorithm, the entire aorta mesh is updated ( Fig.12). Then the updated region of interest is selected for computation. Provided effors are made to increase the mesh quality, this algorithm is believed to be able to provide real-time realistic estimates of interaction forces and stresses. Initially the focus would lie on the region around the catheter tip. In a later stage larger contact areas would be computed.

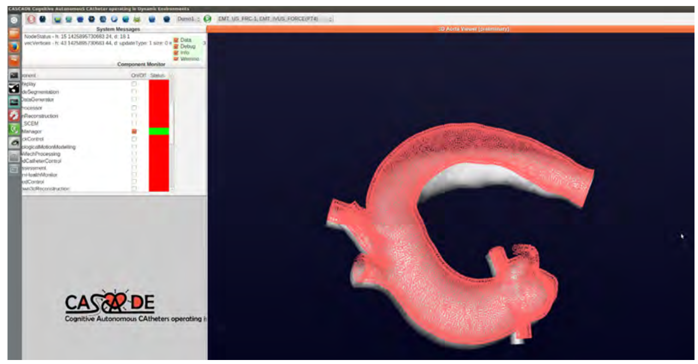

Fig. 12. Real-time update of aorta mesh accounting for global deformation; input is here an updated geometric model (aorta center-line) e.g. obtained from SCEM. The original aorta mesh is depicted in grey; overlay of mesh in red.

### 5.5. *Detection of risk prone areas*

Regions with plaque or calcification deposits, risk prone areas that are highly complex and difficult to model are better avoided all together. Based on estimates of the location of these areas e.g. from pre-operative computer tomography (CT), safer trajectories around such areas could be planned. Alternatively it is possible to use the embedded sensors to directly measure and steer around these areas.

Related to the first approach, different approaches for detecting calcification in CT images based on supervised machine learning were considered. With the so-called pixel-wise approach, each pixel in the image is treated separately as a sample that is classified based on statistical properties from the local neighbourhood. A classifier such as a support vector machine (SVM) can be used here. In contrast, with a segment-wise approach, the image is over-segmented. Similar pixels are clustered prior to feature extraction. Each segment is then classified as a whole. The simple linear iterative clustering (SLIC)[64] technique has been investigated. SLIC can be tuned by selecting an appropriate amount and an appropriate level of compactness of the segments. In general, over-segmentation reduces the amount of training samples needed to train the classifier. Instead of classifying pixels, whole segments are treated as input for the classifier. The distribution of intensity values in the segment is used as property. Calcified segments with high intensity values are separated from non-calcified ones with low intensity values. The classification is done on each CT slice separately by an SVM with a linear kernel. With the transformation matrix embedded in the CT slices, the points of detected calcification are projected into 3D space. The true predicted calcifications are shown in Fig.13 along with the mesh that is generated out of the same CT data.

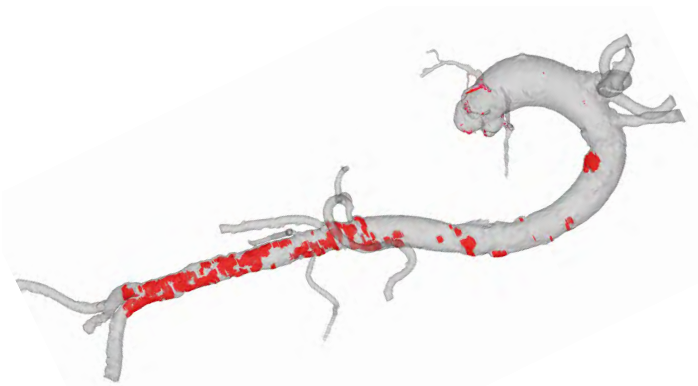

Fig. 13. True positive calcification in 3D aorta mesh.

Through appropriate registration or intra-operative modeling techniques such as described in SubSec.5.1 and SubSec.5.3 the predicted calcification regions could be updated estimating the intra-operative distribution.

Alternatively, risk prone areas can be measured directly, e.g. through intravascular ultrasound. In fact, IVUS is considered as the gold standard to detect calcifications[65] (see also Fig.5(f)). Further, it is clinically known that plaques within the aorta are more likely to occur in close proximity to its branches.[66,67] Branch detection and automatic highlighting thereof could help increase the awareness of these risky areas. Previous approaches in branch detection in IVUS images and sequences have used shape-driven methods[68] and classification techniques.[69] However, these have mainly focused on the coronary arteries. Intra-operative use of such segmentation and classifiers is difficult due to their computational complexity. In the CASCADE framework, the focus has been on devising effective branch detection methods based on the lumen shape and the Radon transform. The methods are computationally inexpensive and allow for real-time processing on IVUS images that are obtained anyway as the robotic catheter advances towards the aortic valve.

## 6. Skill assessment and planning

A direct translation of the available geometric, mechanic and anatomic information towards adequate steering actions is difficult to achieve. The catheter invariably follows a complex path, whereby it is often impossible to avoid touching some risky areas. Through long years of training, experienced interventionalists have learned to understand which areas can be contacted and what level of contact is acceptable. It is crucial that an autonomous system possesses a similar skill allowing it to make these same trade-offs in a sensible and timely manner. In an attempt to capture this knowledge a teleoperation system has been built (described in 6.1) to allow intuitive steering of the catheter and to allow recording of the commanded steering actions. This information can then be used to evaluate the surgical skill (SubSec.6.3). By attaching the correct surgical episode to a certain set of actions (SubSec.6.2) this information can be put in context and as thus made more specific.

### 6.1. *Teleoperation control and guidance*

Several works have dealt with catheter teleoperation control in the past. Departing from a given mapping between master and catheter DoFs, these works propose methods to realize the said mapping so that the respective slave DoFs track the corresponding master DoFs as close as possible.[35,70] Little discussion took place as to which mapping is good to start with. Especially when it concerns steering complex multi-DoF catheters in highly dynamic environments this is an important question. Active catheters typically combine proximal and distal actuation DoFs. But the reference frame in which the distal section is defined is constantly moving and rotating while the catheter is inserted. Tracking the motion of this distal section imposes a significant mental load upon the surgeon. In contrast to the CASCADE catheters, current manual interventions offer limited maneuverability over the catheter's distal DoFs. Existing commercial robotic systems are not designed either for working in such coordinated and dynamic fashion. Next to the question how to intuitively map the user's steering commands, the question arises how the available information can be offered to the user such that he/she can take full advantage of it, allowing him/her to steer the catheter with confidence in 3D space.

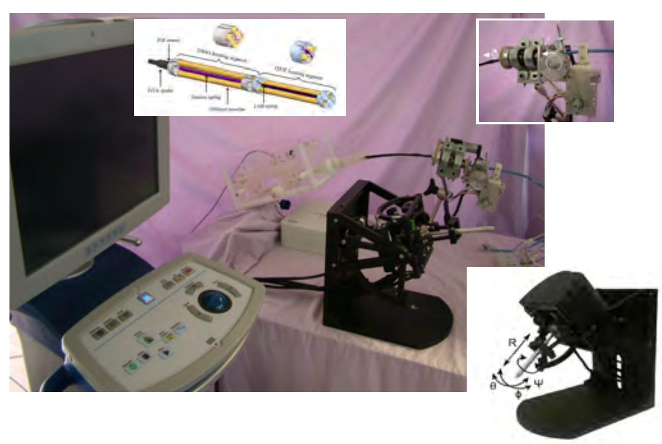

Fig. 14. View on basic teleoperation setup that has been used to investigate intuitive and efficient catheter steering strategies.

To answer the first question, a teleoperation setup was built as depicted in Fig.14. The system consists of a 2-DoF catheter driver controlling insertion and roll of a catheter with 2 pairs of antagonistic fluidic muscles at the tip (2 distal DoFs). An in-house built 4-DoF haptic joystick[71] steers the catheter DoFs. Although theoretically possible, clinicians advised against using the roll-DoF as such motion would entail a large intrinsic contact with the vasculature, with consequent risks for plaque or calcium dislodgement.

In first instance three 3-DoF mappings $M1$, $M2$, $M3$ between master and slave DoFs were tested and compared.[43] In $M1$ three joystick DoFs are mapped to the insertion (rate control) and the pairs of antagonistic muscles. In $M2$ the distal bending plane (in which bending takes place) and amplitude are controlled independently. This requires proper coordinated control of the distal muscles. The rationale behind $M2$ is that the catheter curvature is more or less constant at the aortic arch, so that passing the arch would require less user input. $M3$ takes into account the roll motion that the catheter experiences while entering the vessel. This roll re-orients the distal reference frame of the pair of antagonistic muscles. Roll is available through the 6-DoF EMT sensor that is embedded in the catheter tip. It is then compensated for so that catheter tip bending will be always take place in the same manner.

Experiments were carried out by an expert endovascular surgeon.[43] Multiple insertions were done in a flexible aorta model. The experiments show that the user performs better with $M2$, both in terms of time to reach the aortic valve ($p = 0.03$), length of path ($p = 0.01$) and smoothness of the movements ($p = 0.03$). Further experiments will evaluate positioning and alignment tasks in greater detail.

Experiments are ongoing to answer which haptic and visual guidance cues are preferable and simplify catheter steering task. Fig.15 gives an overview of a few visualisation screens the user gets access to.

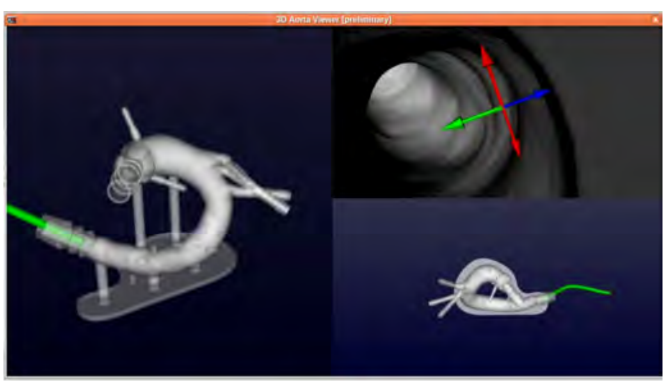

Fig. 15. Visualisation of catheter experiment in rigid testbed of Fig.5(b). Available 3-dimensional information allows generation of views from different perspectives including generation of an endoscopic view (right up). The entire catheter shape can be displayed using the catheter reconstruction from SubSec.5.2. Arrows in endoscopic view show how joystick input would result in motion of the catheter tip.

## 6.2. *Episode segmentation*

Optimal assistance depends on the specific context. Control objectives vary as the procedure progresses. For fully autonomous motion the controller should thus understand, account for and automatically adapt to the circumstances. A detailed analysis of the surgical workflow lies at the base of such cognitive system. Segmentation and identification of surgical episodes or tasks can alert the surgeon intra-operatively for difficult or risky areas within particular surgical steps. This can facilitate intra-operative catheter control and decision making, helping to safely navigate through a fragile and dynamic environment in the presence of large uncertainty about its properties. The analysis of the surgical tasks can further help to quantitatively evaluate surgical skill making the link to specific episodes.

Thus far, the analysis of surgical workflow has been extensively studied for minimally invasive procedures. Surgical tools,[72] visual and anatomical cues[73] as well as kinematic data[74] have been used to recognise surgical phases and actions. For cardiovascular procedures workflow analyses have been scarce. The workflow of the TAVI procedure was segmented by expert endovascular surgeons into 10 surgical tasks including the placement of a pacing catheter and a guidewire in the femoral vein, the introduction of an introducer sheath, the pre-dilation of the valve with a balloon, the delivery of the artificial valve and the evaluation of the valve positioning. The surgical task that was focused on was the 'Delivery of the aortic valve' (the $8^{\text{th}}$ task in line) given its central role within the procedure. This task has been further segmented into 6 sequential surgical gestures: (1) catheter pushed up the descending aorta, (2) catheter pushed around the aortic arch, (3) catheter pushed down the ascending aorta, (4) catheter pulled-back in the ascending aorta, (5) catheter pulled-back in the aortic arch, (6) catheter pulled-back in the descending aorta.

An on-line approach for surgical gesture recognition has been developed.[75] Descriptive Curve Coding (DCC) was used to represent the 3D motion of the catheter in the aorta with a set of motion words. To enable early recognition of partially-observed gestures, integral histograms of the motion words are generated to describe a surgical task. The 'dynamic bag-of-words' approach has been used to recognise surgical gestures, based on dynamic matching of integral histograms considering the sequential nature of gestures during surgical tasks. Detailed validation with phantom data has been performed. The results derived justify the potential clinical value of the technique.[75]

## 6.3. *Skill assessment*

Sec. 2.1 outlined the challenges and risks of TAVI procedures. A robotic system must replicate the performance of an expert endovascular surgeon demonstrate its capability to deal with these challenges and risks. By assessing surgical skills quantitatively, the technical knowledge of how an expert surgeon performs a TAVI operation can be conveyed to the robot for this purpose.

To achieve this, a novel system to evaluate surgical skills is developed under CASCADE. Traditional methods for evaluating surgical expertise consist out of written and oral examinations, monitoring by experts of performance during sessions on cadavers, animals, inanimate models or virtual simulators. Assessment takes place using standardized grading scales or checklists. All methods require an expert to observe and assign grades as the trainee executes a phantom operation. Overall supervised assessment is inefficient in terms of time and resources required, as well as subjective. Recent studies in laparoscopic minimally invasive surgery suggest that the motion pattern of surgical instruments can be indicative of surgical competence.[76] Inspired by this, we attempt to expand this analysis for endovascular procedures and particularly TAVI.

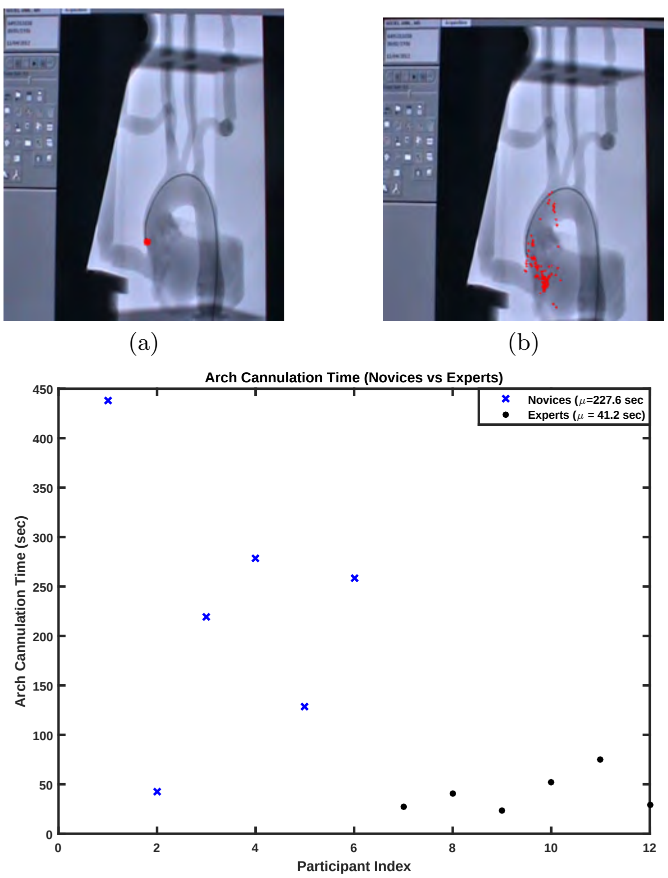


(c)

Fig. 16. Preliminary investigation; (a) Tracking of catheter tip; (b) Catheter tip tajectory; (c) Cannulation times of the aortic arch for 6 novices ($\mu$ = 227.6$sec$) - 6 experts ($\mu$ = 41.2$sec$). Experts perform more efficiently.

In principle, expert surgeons focus on three key technical areas during manual assessment of endovascular trainees: 1) instrument handling and flow of operation; 2) respect for tissue/ danger for damage; 3) use of imaging modalities. Skilled surgeons operate surgical instruments in a smooth continuous way without jerky and unnecessary movements. They demonstrate dexterity and are also aware of the amount of force they exercise to the catheters tip, when approaching sensitive areas of the vasculature (calcifications, vessel wall and lesions) and ensure that no danger appears for calcium dislodgement or vessel rupture.

Through appropriate processing the objective is to produce quantitative metrics that represent these three technical areas and can provide analogous information from which surgical skill can be assessed. The novel catheter and developed image and tracking algorithms can provide the necessary information for accomplishing this.

Whereas in future work, CASCADE-enabled steering mechanisms can be treated and evaluated, the aim at this stage is to acquire as much as possible information from observing traditional interventions. Specifically, tracking the catheter/guidewire in fluoroscopy images and the motion relative to the vessel wall and the calcifications, will allow evaluating the smoothness of motion, by analysing kinematic properties such as acceleration and jerk. It will also give insight on safe navigation, away from the risky areas. Additional measures from the utilization of the imaging modalities (fluoroscopy time, amount of contrast agent used) combined with the kinematic properties will form a basis for developing an objective method for evaluating surgical skill. Preliminary results from a study where both experts and novice surgeons performed aortic arch cannulation, on a silicon phantom model in which the catheters tip was tracked in the video sequence, reveal that experts handle the catheter in a more efficient way resulting in faster cannulation of the aortic arch, as illustrated in Fig.16.

## 7. Advanced Control

### 7.1. *Control of continuum robots*

Given the difference in bandwidth between the distal fluidic actuated tip and the other catheter DoFs in first instance an approach was developed that focuses on the control of the distal part of the catheter while making abstraction of the catheter tail. Since the distal part has a large compliance it was modelled with a Cosserat rod model. In previous work we developed fast computation schemes to obtain the Jacobian and Compliance matrices of such continuum robots.[77] Here, we investigated means to use these models to reach good position and force control necessary to precisely position a valve implant.

To demonstrate the validity of the adopted model the distal catheter is mounted via a force sensor on top of an industrial robot (LWR, KUKA). A constraint-based task formalism[78] was adopted to incorporate a plurality of relevant objectives. Here, the flexible link and rigid robot were controlled jointly so as to apply a reference force, while maintaining a position constraint. Such position could present a strategic location in the aorta e.g. selected to prevent the catheter to contact a risk zone area.

Figure 17 shows the setup and the experimental results. The robot is commanded to move from an unloaded configuration at $t = 0\,s$ in contact with the wall (black line) to a loaded configuration ($t = 20\,s$, dashed black line) while the center-line of the mounting frame is maintaining a position constraint. The graph shows that a desired force can be applied (bottom), while the position constraint can be held quite accurately (error shown in lower graph). It can be seen that the orientation of the catheter (which is not constrained) varies to a large extent. This implies that if a certain force is to be exerted the resulting deformation of the catheter tip is to be accounted for.

Current investigations focus on tailoring the method to control the distal part of the catheter in the ascending aorta. A safe *landing* zone at the aortic wall could serve here as the base for the active distal catheter. Such approach seems natural as it turns out that there is little variation in how catheters enter and pass through the aortic arch itself. Expanding the Cosserat rod model to describe the catheter over its entire length is not straightforward as this would require knowledge of all interaction forces over the entire catheter length. Given the absence of a tactile skin appropriate for this purpose, efforts are geared to estimate forces from shape or simulation.

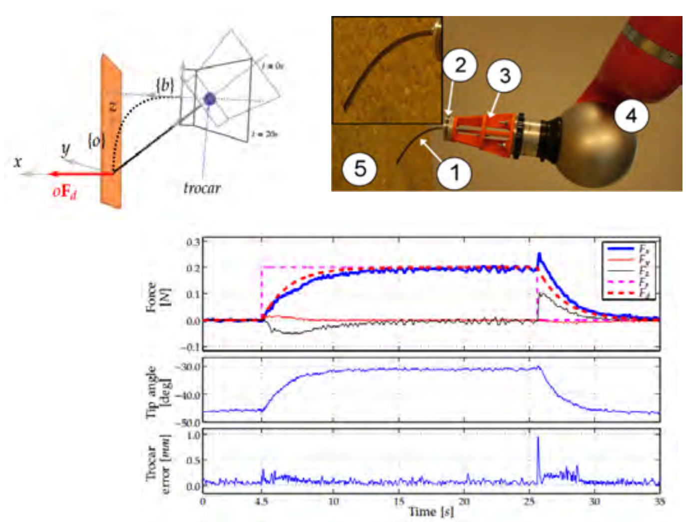


Fig. 17. Experimental control setup - flexible link ① represents the catheter distal section, mounted on ATI force sensor ②, attached to KUKA LWR ④ via mounting stage ③. The robot pushes a foamy surface ⑤; close-up of flexible link in upper left corner. The upper graph shows the interaction force between the tip and the wall as a desired force step is commanded; middle graph: evolution of tip orientation; bottom graph: position error of the positioning constraint.

## 7.2. *Autonomous catheter control - minimum-energy approach*

Obtaining an accurate kinematic map of robotic catheters that are evolving in a constrained environment requires detailed knowledge of all interactions between the robot and the environment. Such interactions are complex, intrinsically distributed and depend on the properties of both catheter and environment. In the absence of adequate tactile skins, an approach based on a quasi-static predictive model was developed.[31] The method follows a minimum energy argumentation to predict changes of catheter shape upon varying robot/catheter actions. A number of input commands are *virtually* applied and corresponding catheter output motions are computed, thus *probing* the input-output space. From this the differential kinematics under the form of a Jacobian matrix is derived. This matrix is then used in the controller to estimate the appropriate input command for a desired output motion.

Fig.18 shows the outcome of a successful control experiment in a 2-dimensional rigid mockup. Deviation from the target trajectory, here the vessel centerline, can be explained by limitations in accuracy of the shape sensing used in the feedback loop of the controller. A larger contribution comes however from physical limitations of the employed hardware namely the limited bending angle of the catheter. A full insertion takes 734s. The experiment was conducted in a two-dimensional environment since this makes it easier to compute the error from the targeted path. Similar results (and computation times) were obtained from experiments conducted in the virtual reality simulator in 3D.

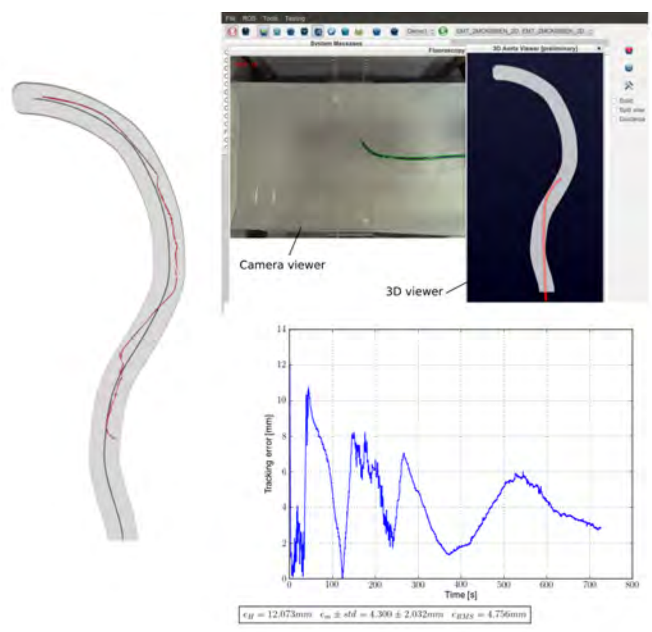


Fig. 18. In-vitro experiment of autonomous catheter navigation in 2D rigid mock-up. Catheter with single bending segment and bending angle limited to [−55°;50°]. [right up] View on CASCADE platform. The camera viewer displays the detected catheter contours and centerline (green lines). The catheter centerline is registered to the mesh coordinate frame and sent to the minimum energy model and associated controller. The registered catheter shape visible as red tube in 3D viewer; [left] tip position (red line) and target path (black line); [bottom] Tracking errors: Hausdorff error, mean error and standard deviation, and RMS error respectively: $e_{\mathrm{h}}$=12.073mm, $e_{\mathrm{m}} \pm$ std=4.0 $\pm$ 2.032 mm and $e_{\mathrm{rms}}$=4.756mm.

### 7.3. *Autonomous catheter control: a data-driven approach*

Machine learning techniques can be adopted to learn the input-output behaviour of the catheter inside vessels of artificial mock-ups directly from the data. A data-based catheter steering method was proposed and tested through a 2D deformable aorta mock-up and a catheter drive system. Whereas the methods have been applied on a cable-driven catheter TactiCath™(SJMG), the proposed approaches are more general and would transfer also to the McKibben-based or other actuation systems.

The catheter is modelled using joint probability densities, which are represented by mixture of Gaussians. A Dynamic Gaussian Mixture Model (DGMM) served for probabilistic representation. DGMM is the extended version of the standard Gaussian Mixture Model (GMM), which allows dynamic variation of the number of Gaussian components in the model.[79] This helps capturing multiple relationships among variables of the catheter model. Additionally, the online methods implemented in DGMM allow updating the model incrementally as more data is acquired, making DGMM a good candidate for a system that learns continuously. During training of the joint probability distribution, different features of the catheter such as the catheter tip position, the catheter shape and the bending angle are captured and used as input data to the model. The trained model and steering approach are tested by a centerline following experiment in a 2D deformable aorta mock-up. The detected features of the catheter and the experimental results are shown in Fig. 19. The euclidean distance error of the catheter tip is typically between 0 mm and 6 mm, except for a time interval with an error of up to 12.2 mm. This could be caused by the friction and interaction between the catheter and the mock-up. The mean euclidean distance error is 7.63mm.

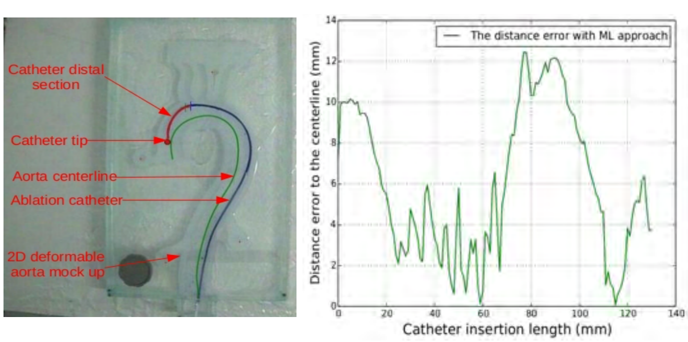


Fig. 19. In-vitro experiment of autonomous catheter navigation in a 2D deformable mock-up, with single bending segment and bending angle limited to [15°;70°]. [left] The camera image displays the detected catheter distal section (red line), catheter tip (red dot), catheter body (blue line) and aorta centerline (green line); [right] The tracking error is calculated between the catheter tip and the aorta centerline after each steering action.

## 8. Conclusions and future work

Advances in miniaturized surgical instrumentation are key to less demanding and safer medical interventions. This paper aims to report on the progress that was made within the EU-funded CASCADE project towards autonomous catheter steering. Without being exhaustive, progress is sketched in terms of individual building blocks, key supporting technologies for autonomous catheter steering: catheter design, vessel reconstruction, catheter shape modeling, surgical skill analysis, decision-making and control.

Future efforts will be devoted to unite the efforts in different sub-domains moving to experiments and validation of steering capability in more complex settings that fully incorporate the challenges imposed by the hemodynamics. The investment in carefully tailored software framework and set of testbeds is expected to pay off here particularly.

## References

[1] M. Mirabel, B. Iung, G. Baron, D. Messika-Zeitoun, D. Detaint, J. Vanoverschelde, E. Butchart, P. Ravaud, and A. Vahanian, “What are the characteristics of patients with severe, symptomatic, mitral regurgitation who are denied surgery?” *Eur Heart Journal*, vol. 28, no. 11, pp. 1358–1365, Mar 2007.

[2] M. B. Leon, C. R. Smith, M. Mack, D. C. Miller, J. W. Moses, L. G. Svensson, E. M. Tuzcu, J. G. Webb, G. P. Fontana, R. R. Makkar *et al.*, “Transcatheter aortic-valve implantation for aortic stenosis in patients who cannot undergo surgery,” *New England Journal of Medicine*, vol. 363, no. 17, pp. 1597–1607, 2010.

[3] C. R. Smith, M. B. Leon, M. J. Mack, D. C. Miller, J. W. Moses, L. G. Svensson, E. M. Tuzcu, J. G. Webb, G. P. Fontana, R. R. Makkar *et al.*, “Transcatheter versus surgical aortic-valve replacement in high-risk patients,” *New England Journal of Medicine*, vol. 364, no. 23, pp. 2187–2198, 2011.

[4] R. R. Makkar, G. P. Fontana, H. Jilaihawi, S. Kapadia, A. D. Pichard *et al.*, “Transcatheter aortic-valve replacement for inoperable severe aortic stenosis,” *New England Journal of Medicine*, vol. 366, no. 18, pp. 1696–1704, 2012.

[5] L. Kohn, J. Corrigan, and M. Donaldson, *To err is human: building a safer health system.* Washington: National Academy Press, 2000.

[6] R. Morena, L. Calvo, P. Salinas, D. Dobarro, J. Santiago, A. Sanchez-Recalde, G. Galeote, L. Riera, I. Moreno-Gomez, J. Mesa, I. Plaza, and J. Lopez-Sendon, “Causes of peri-operative mortality after transcatheter aortic valve implantation: A pooled analysis of 12 studies and 1,223 patients,” *J INVASIVE CARDIOL*, vol. 23, pp. 180–184, 2011.

[7] G. Tarantini, V. Gasparetto, M. Napodano, C. Fraccaro, G. Gerosa, and G. Isabella, “Valvular leak after transcatheter aortic valve implantation: a clinician update on epidemiology, pathophysiology and clinical

implications," *American journal of cardiovascular disease*, vol. 1, no. 3, p. 312, 2011.
[8] A. Ghanem, A. Müller, C. P. Nähle, J. Kocurek, N. Werner, C. Hammerstingl, H. H. Schild, J. O. Schwab, F. Mellert, R. Fimmers *et al.*, "Risk and fate of cerebral embolism after transfemoral aortic valve implantation: a prospective pilot study with diffusion-weighted magnetic resonance imaging," *Journal of the American College of Cardiology*, vol. 55, no. 14, pp. 1427–1432, 2010.
[9] D. S. Bach, J. I. Radeva, H. G. Birnbaum, A.-A. Fournier, and E. G. Tuttle, "Prevalence, referral patterns, testing, and surgery in aortic valve disease: leaving women and elderly patients behind?" *The Journal of heart valve disease*, vol. 16, no. 4, pp. 362–369, 2007.
[10] C. M. Otto, "Timing of aortic valve surgery," *Heart*, vol. 84, no. 2, pp. 211–218, 2000.
[11] B. Iung, G. Baron, E. G. Butchart, F. Delahaye, C. Gohlke-Bärwolf, O. W. Levang, P. Tornos, J.-L. Vanoverschelde, F. Vermeer, E. Boersma *et al.*, "A prospective survey of patients with valvular heart disease in europe: The euro heart survey on valvular heart disease," *European heart journal*, vol. 24, no. 13, pp. 1231–1243, 2003.
[12] E. Charlson, A. T. Legedza, and M. B. Hamel, "Decision-making and outcomes in severe symptomatic aortic stenosis," *Journal of Heart Valve Disease*, vol. 15, no. 3, p. 312, 2006.
[13] A. Kasel, S. Cassese, A. Leber, W. von Scheidt, and A. Kastrati, "Fluoroscopy-guided aortic root imaging for TAVR: 'Follow the Right Cusp' rule," *JACC: Cardiovascular Imaging*, vol. 6, no. 2, pp. 274 – 275, 2013.
[14] J. Plotkin, R. Siegel, and R. Beigel, "Plaque disruption during transcatheter aortic valve replacement," *Eur. Heart J. Cardiovasc. Imaging*, vol. 15, no. 1, pp. 117–117, Jan 2014.
[15] A. Aminian, J. Lalmand, and B. El Nakadi, "Perforation of the descending thoracic aorta during transcatheter aortic valve implantation (tavi): An unexpected and dramatic procedural complication," *Catheterization and Cardiovascular Interventions*, vol. 77, no. 7, pp. 1076–1078, 2011.
[16] J. G. Webb, S. Pasupati, L. Achtem, and C. R. Thompson, "Rapid pacing to facilitate transcatheter prosthetic heart valve implantation," *Catheterization and cardiovascular interventions*, vol. 68, no. 2, pp. 199–204, 2006.
[17] J. Bonatti, G. Vetrovec, C. Riga, O. Wazni, and P. Stadler, "Robotic technology in cardiovascular medicine," *Nature Reviews Cardiology*, vol. 11, no. 5, pp. 266–275, 2014.
[18] H. Rafii-Tari, C. J. Payne, and G.-Z. Yang, "Current and emerging robot-assisted endovascular catheterization technologies: A review," *Annals of biomedical engineering*, vol. 42, no. 4, pp. 697–715, 2014.
[19] V. Meiser and D. Seatovic, "System integration: A comparison of the scath and the cascade system architecture," in *Proceedings of the 3rd Joint Workshop on New Technologies for Computer - Robot Assisted Surgery*, 11-13 Sep. 2013 2013, pp. 130–133.
[20] V. Luboz, R. Blazewski, D. Gould, and F. Bello, "Real-time guidewire simulation in complex vascular models," *Vis. Comput.*, vol. 25, pp. 827–834, 2009.
[21] F. Wang, L. Duratti, E. Samur, U. Spaelter, and H. Bleuler, "A computer-based real-time simulation of interventional radiology." in *Conf Proc IEEE Eng Med Biol Soc*, 2007.
[22] S. Cotin, C. Duriez, J. Lenoir, P. Neumann, and S. Dawson, "New approaches to catheter navigation for interventional radiology simulation," in *Proceedings of the 8th international conference on Medical image computing and computer-assisted intervention - Volume Part II*, ser. MICCAI'05. Berlin, Heidelberg: Springer-Verlag, 2005, pp. 534–542.
[23] S. Li, J. Qin, J. Gao, Y.-P. Chui, and P.-A. Heng, "A novel fem-based numerical solver for interactive catheter simulation in virtual catheterization," *Journal of Biomedical Imaging*, vol. 2011, p. 3:3, 2011.
[24] W. Tang, P. Lagadec, D. Gould, T. Wan, J. Zhai, and T. How, "A realistic elastic rod model for real-time simulation of minimally invasive vascular interventions," *Vis. Comput.*, vol. 26, no. 9, pp. 1157–1165, 2010.
[25] M. Konings, E. Kraats, T. Alderliesten, and W. Niessen, "Analytical guide wire motion algorithm for simulation of endovascular interventions," *Medical and Biological Engineering and Computing*, vol. 41, no. 6, pp. 689–700, 2003.
[26] T. Alderliesten, M. Konings, and W. Niessen, "Simulation of minimally invasive vascular inventions for training purposes," *Comput Aided Surg*, vol. 9, no. 1–2, pp. 3–15, 2004.
[27] ——, "Robustness and complexity of a minimally invasive vascular intervention simulation system," *Medical Physics*, vol. 33, no. 12, pp. 4758–4769, 2006.
[28] T. Alderliesten, P. A. N. Bosman, and W. Niessen, "Towards a real-time minimally-invasive vascular intervention simulation system," *Medical Imaging, IEEE Transactions on*, vol. 26, no. 1, pp. 128–132, 2007.
[29] T. Alderliesten, M. Konings, and W. Niessen, "Modeling friction, intrinsic curvature, and rotation of guide wires for simulation of minimally invasive vascular interventions," *Biomedical Engineering, IEEE Transactions on*, vol. 54, no. 1, pp. 29–38, 2007.
[30] P. Tran, A. Devreker, G. Smoljkic, H. De Praetere, E. Vander Poorten, and J. Vander Sloten, "Patient-specific design of multi-component steerable catheters," in *Proc. of 3rd Joint Workshop on New Technologies for Computer - Robot Assisted Surgery*, 2013, pp. 37–40.
[31] P. Tran, E. Vander Poorten, G. Smoljkic, C. Gruijthuijsen, P. Herijgers, D. Reynaerts, and J. Vander Sloten, "Manipulability of robotic catheters," in *Proc. of 4th Joint Workshop on New Technologies for Computer - Robot Assisted Surgery*, 2014, pp. 135–138.

[32] A. Tibebu, B. Yu, Y. Kassahun, E. Vander Poorten, and P. Tran, "Towards autonomous robotic catheter navigation using reinforcement learning," in *Proc. 4th Joint Workshop on New Technologies for Computer - Robot Assisted Surgery*, 2014, pp. 163–166.

[33] G. Biglino, P. Verschueren, R. Zegels, A. M. Taylor, and S. Schievano, "Rapid prototyping compliant arterial phantoms for in-vitro studies and device testing," *J Cardiovasc Magn Reson*, vol. 15, no. 2, pp. 1–7, 2013.

[34] G. Srimathveeravalli, T. Kesavadas, and X. Li, "Design and fabrication of a robotic mechanism for remote steering and positioning of interventional devices," *The International Journal of Medical Robotics and Computer Assisted Surgery*, vol. 6, no. 2, pp. 160–170, 2010.

[35] S. Kesner and R. Howe, "Position control of motion compensation cardiac catheters," *Robotics, IEEE Transactions on*, vol. 27, no. 6, pp. 1045–1055, 2011.

[36] ——, "Robotic catheter cardiac ablation combining ultrasound guidance and force control," *The International Journal of Robotics Research*, 2014.

[37] G. J. Vrooijink, T. T. Ellenbroek, P. Breedveld, J. G. Grandjean, and S. Misra, "A preliminary study on using a robotically-actuated delivery sheath (rads) for transapical aortic valve implantation," in *IEEE Int. Conf. Robot. Autom. (ICRA'14)*, 2014, pp. 4380–4386.

[38] T. Fukuda, S. Guo, K. Kosuge, F. Arai, M. Negoro, and K. Nakabayashi, "Micro active catheter system with multi degrees of freedom," in *Robotics and Automation, 1994. Proceedings., 1994 IEEE International Conference on*, may 1994, pp. 2290 –2295 vol.3.

[39] J. Jayender, R. V. Patel, and S. Nikumb, "Robot-assisted active catheter insertion: algorithms and experiments," *The International Journal of Robotics Research*, vol. 28, no. 9, pp. 1101–1117, 2009.

[40] Y. Fu, H. Liu, W. Huang, S. Wang, and Z. Liang, "Steerable catheters in minimally invasive vascular surgery," *The International Journal of Medical Robotics and Computer Assisted Surgery*, vol. 5, no. 4, pp. 381–391, 2009.

[41] K. Ikuta, H. Ichikawa, and K. Suzuki, "Safety-active catheter with multiple-segments driven by micro-hydraulic actuators," in *Medical Image Computing and Computer-Assisted Intervention MICCAI 2002*, ser. Lecture Notes in Computer Science, T. Dohi and R. Kikinis, Eds. Springer Berlin Heidelberg, 2002, vol. 2488, pp. 182–191.

[42] A. Devreker, E. Vander Poorten, P. Tran, H. De Praetere, P. Herijgers, J. Vander Sloten, and D. Reynaerts, "Towards fluidic actuation for catheter-based interventions," in *Proceedings Actuator 2014*, Bremen, Germany, 2014, pp. 173–176.

[43] B. Rosa, A. Devreker, H. De Praetere, C. Gruijthuijsen, S. Portoles-Diez, A. Gijbels, D. Reynaerts, P. Herijgers, J. Vander Sloten, and E. Vander Poorten, "Intuitive teleoperation of active catheters for endovascular surgery," in *Intelligent Robots and Systems, 2015. (IROS 2015). Proceedings. 2015 IEEE/RSJ International Conference on*, 2015, p. accepted for publication.

[44] A. Devreker, B. Rosa, A. Desjardins, E. Alles, L. Garcia-Peraza, E. Maneas, D. Stoyanov, T. Vercauteren, A. David, J. Deprest, S. Ourselin, D. Reynaerts, and E. Vander Poorten, "Fluidic actuation for intra-operative in situ imaging," in *Intelligent Robots and Systems, 2015. (IROS 2015). Proceedings. 2015 IEEE/RSJ International Conference on*, 2015, p. accepted for publication.

[45] B. A. Childers, D. K. Gifford, R. G. Duncan, M. T. Raum, M. E. Vercellino, and M. E. Froggatt, "Fiber optic position and shape sensing device and method relating thereto," Aug. 24 2010, uS Patent 7,781,724.

[46] C. Shi, S. Giannarou, S. Lee, and G. Yang, "Simultaneous catheter and environment modeling for trans-catheter aortic valve implantation," in *Proceedings of IEEE/RSJ International Conference on Intelligent Robots and Systems (IROS)*, 2014, pp. 2024–2029.

[47] C. Tekes, T. Xu, and F. Degertekin, "Improved fl-ivus imaging with low voltage single-chip cmut-on-cmos array using temporally coded excitation," in *Ultrasonics Symposium (IUS), 2014 IEEE International*, Sept 2014, pp. 1308–1311.

[48] J. Sra and S. Ratnakumar, "Cardiac image registration of the left atrium and pulmonary veins," *Heart Rhythm*, vol. 5, no. 4, pp. 609 – 617, 2008.

[49] Z. J. Malchano, P. Neuzil, R. C. Cury, G. Holmvang, J. Weichet *et al.*, "Integration of cardiac ct/mr imaging with three-dimensional electroanatomical mapping to guide catheter manipulation in the left atrium: Implications for catheter ablation of atrial fibrillation," *J. of Cardiovasc. Electrophysiol.*, vol. 17, no. 11, pp. 1221–1229, 2006.

[50] J. Dong, T. Dickfeld, D. Dalal, A. Cheema, C. R. Vasamreddy *et al.*, "Initial experience in the use of integrated electroanatomic mapping with three-dimensional mr/ct images to guide catheter ablation of atrial fibrillation," *J. of Cardiovasc. Electrophysiol.*, vol. 17, no. 5, pp. 459–466, 2006.

[51] T. W. G. Carrell, B. Modarai, J. R. I. Brown, and G. P. Penney, "Feasibility and limitations of an automated 2d-3d rigid image registration system for complex endovascular aortic procedures," *Journal of Endovascular Therapy*, vol. 17, no. 4, pp. 527–533, 2010.

[52] H. Zhong, T. Kanade, and D. Schwartzman, "Virtual touch: An efficient registration method for catheter navigation in left atrium," in *Medical Image Computing and Computer-Assisted Intervention*, 2006, pp. 437–444.

[53] C. Gruijthuijsen, B. Rosa, P. Tran, J. Vander Sloten, E. Vander Poorten, and D. Reynaerts, "An automatic registration method for radiation-free catheter navigation guidance," *Journal of Medical Robotics Research*, 2015 (submitted).

[54] C. Papazov and D. Burschka, "Stochastic global optimization for robust point set registration," *Computer Vision and Image Understanding*, vol. 115, no. 12, pp.

1598 – 1609, 2011.

[55] P. Chang, A. Rolls, C. Riga, C. Bicknell, and D. Stoyanov, “A b-spline tube model for catheter and guidewire tracking,” in *Proceedings of the 4th Joint Workshop on New Technologies for Computer - Robot Assisted Surgery*, 2014, pp. 41–43.

[56] C. Bibby and I. Reid, “Robust real-time visual tracking using pixel-wise posteriors,” in *European Conference on Computer Vision*, 2008, pp. 831–844.

[57] E. Lugez, H. Sadjadi, D. R. Pichora, R. E. Ellis *et al.*, “Electromagnetic tracking in surgical and interventional environments: usability study,” *International Journal of Computer Assisted Radiology and Surgery*, 2014.

[58] A. M. Franz, T. Haidegger, W. Birkfellner, K. Cleary *et al.*, “Electromagnetic tracking in medicine -A review of technology, validation, and applications,” *IEEE Transactions on Medical Imaging*, vol. 33, no. 8, pp. 1702–1725, 2014.

[59] R. Tilz, K. Chun, A. Metzner, A. Burchard, E. Wissner, B. Koektuerk, M. Konstantinidou, D. Nuyens, T. De Potter, K. Neven, A. Furnkranz, F. Ouyang, and B. Schmidt, “Unexpected high incidence of esophageal injury following pulmonary vein isolation using robotic navigation,” *Journal of Cardiovascular Electrophysiology*, vol. 21, no. 8, p. Tilz10, August 2010.

[60] J. Gregson, A. Sheffer, and E. Zhang, “All-hex mesh generation via volumetric polycube deformation,” in *Computer graphics forum*, vol. 30, no. 5. Wiley Online Library, 2011, pp. 1407–1416.

[61] K. Miller, G. Joldes, D. Lance, and A. Wittek, “Total lagrangian explicit dynamics finite element algorithm for computing soft tissue deformation,” *Communications in Numerical Methods in Engineering*, vol. 23, no. August 2006, pp. 121–134, 2007.

[62] V. Strbac, J. Vander Sloten, and N. Famaey, “Analysing the potential of gpgpus for real-time explicit finite element analysis of soft tissue deformation using cuda,” *Finite Elements in Analysis and Design*, accepted for publication, 2015.

[63] T. C. Gasser, R. W. Ogden, and G. A. Holzapfel, “Hyperelastic modelling of arterial layers with distributed collagen fibre orientations,” *Journal of the royal society interface*, vol. 3, no. 6, pp. 15–35, 2006.

[64] R. Achanta, A. Shaji, K. Smith, A. Lucchi, P. Fua, and S. Ssstrunk, “SLIC Superpixels Compared to State-of-the-art Superpixel Methods,” *IEEE Transactions on Pattern Analysis and Machine Intelligence*, 2012.

[65] A. H. Ben, K. Bouzouita, I. Hamdi, A. Mokaddem, A. Y. Ben, and M. Boujnah, “Comparison of coronary calcifications detection by angiogram versus intravascular ultrasound.” *La Tunisie medicale*, vol. 91, no. 3, pp. 196–199, 2013.

[66] G. D. Giannoglou, A. P. Antoniadis, K. C. Koskinas, and Y. S. Chatzizisis, “Flow and atherosclerosis in coronary bifurcations,” *EuroIntervention : journal of EuroPCR in collaboration with the Working Group on Interventional Cardiology of the European Society of Cardiology*, vol. 6 Suppl J, pp. J16–23, December 2010.

[67] O. Arjmandi-Tash, S. E. Razavi, and R. Zanbouri, “Possibility of atherosclerosis in an arterial bifurcation model,” *BioImpacts: BI*, vol. 1, no. 4, p. 225, 2011.

[68] G. Unal, S. Bucher, S. Carlier, G. Slabaugh, F. Tong, and K. Tanaka, “Shape-driven segmentation of the arterial wall in intravascular ultrasound images,” in *IEEE Transactions on Information Technology in Biomedicine*, vol. 12, 2008, pp. 335–347.

[69] M. Alberti, S. Balocco, C. Gatta, F. Ciompi, O. Pujol, J. Silva, X. Carrillo, and P. Radeva, “Automatic bifurcation detection in coronary ivus sequences,” in *IEEE Transactions on Biomedical Engineering*, vol. 59, 2012, pp. 1022–1031.

[70] J. Jayender and R. Patel, “Wave variables based bilateral teleoperation of an active catheter,” in *Biomedical Robotics and Biomechatronics, 2008. BioRob 2008. 2nd IEEE RAS EMBS International Conference on*, Oct 2008, pp. 27–32.

[71] A. Gijbels, E. Vander Poorten, P. Stalmans, H. Van Brussel, and D. Reynaerts, “Design of a teleoperated robotic system for retinal surgery,” in *IEEE International Conference on Robotics and Automation*, 2014.

[72] F. Lalys, D. Bouget, L. Riffaud, and P. Jannin, “Automatic knowledge-based recognition of low-level tasks in ophthalmological procedures,” *International Journal of Computer Assisted Radiology and Surgery*, vol. 8, no. 1, pp. 39–49, 2013.

[73] L. Zappella, B. Bejar, G. Hager, and R. Vidal, “Surgical gesture classification from video and kinematic data,” *Medical Image Analysis*, vol. 17, no. 7, pp. 732–745, 2013.

[74] B. Varadarajan, “Learning and inference algorithms for dynamical system models of dextrous motion,” Ph.D. dissertation, The Johns Hopkins University, 2011.

[75] S. Giannarou, C. Gruijthuijsen, and G. Yang, “Modeling and recognition of ongoing surgical gestures in tavi procedures,” in *Workshop on Modeling and Monitoring of Computer Assisted Interventions (M2CAI), International Conference on Medical Image Computing and Computer Assisted Intervention (MICCAI)*, 2014.

[76] C. Reiley, H. Lin, D. Yuh, and G. Hager, “Review of methods for objective surgical skill evaluation,” *Surgical Endoscopy*, vol. 25, pp. 356–366, 2011, 10.1007/s00464-010-1190-z. [Online]. Available:

[77] G. Smoljkic, D. Reynaerts, J. Vander Sloten, and E. Vander Poorten, “Compliance computation for continuum types of robots,” in *Intelligent Robots and Systems (IROS 2014), 2014 IEEE/RSJ International Conference on*, Sept 2014, pp. 1066–1073.

[78] E. Aertbelien and J. De Schutter, “etasl/etc: A constraint-based task specification language and robot controller using expression graphs,” in *Intelligent Robots and Systems (IROS 2014), 2014 IEEE/RSJ International Conference on*, Sept 2014,

pp. 1540–1546.

[79] M. Edgington, Y. Kassahun, and F. Kirchner, "Using joint probability densities for simultaneous learning of forward and inverse models," in *Proceedings of IEEE IROS International Workshop on Evolutionary and Reinforcement Learning for Autonomous Robot Systems*, 10 2009, pp. 19–22.